Dynamic Sensor-Based Control of Robots with Visual Feedback

LEE E. WEISS, MEMBER, IEEE ARTHUR C. SANDERSON, SENIOR MEMBER, IEEE, AND
CHARLES P. NEUMAN, SENIOR MEMBER, IEEE

Abstract—Sensor-based robot control may be viewed as a hierarchical structure with multiple observers. *Actuator, feature-based,* and *recognition* observers provide the basis for multilevel feedback control at the actuator, sensor, and world coordinate frame levels, respectively. The analysis and design of feature-based control strategies to achieve consistent dynamic performance is addressed. For vision sensors, such an *image-based visual servo* control is shown to provide stable and consistent dynamic control within local regimes of the recognition observer. Simulation studies of two- and three-degree-of-freedom systems show the application of an adaptive control algorithm to overcome unknown and nonlinear relations in the feature to world space mapping.

I. INTRODUCTION

SENSOR-BASED robot control overcomes many of the difficulties of uncertain models and unknown environments which limit the domain of application of current robots used without external sensory feedback. Both industrial arms and mobile robots require sensing capability to adapt to new tasks without explicit intervention or reprogramming. While these relationships between sensing and control have long been recognized in a general sense, the analysis and implementation of specific dynamic control strategies has received relatively little attention. In this paper, we describe the formulation of sensory feedback models for systems which incorporate complex mappings between robot, sensor, and world coordinate frames. These models explicitly address the use of sensory features to define hierarchical control structures, and the definition of control strategies which achieve consistent dynamic performance. Specific simulation studies examine how adaptive control may be used to control a robot based on image feature reference and feedback signals.

Robot control tasks are typically defined in the *world coordinate frame* of the task environment. The environment can include the robot, objects to be manipulated by the robot, and obstacles to be avoided. The control strategy is formulated to map this world frame task definition into control subgoals in other coordinate frames. Hierarchical structures have been suggested for such a system since they facilitate modular organization and efficient decomposition of the task [2]. Fig. 1

illustrates such a hierarchical relationship among coordinate frames, models, and corresponding observers which form the basis for the control strategy. The task definition leads to a control strategy which coordinates the mapping of commands and measurements between levels. The *world* or *global* model includes symbolic representations of objects and relations as well as attributes describing configurations in the world coordinate frame. The *feature* or *local model* includes sensor measurements and derived numerical and symbolic features which are relative to the current (local) system and sensor configuration. The *robot* model describes configurations in robot joint space.

The control strategy for the hierarchical system is based on a set of observers; i.e., sensors and algorithms which relate measured signals to control commands at the various levels. At the robot model level, the *joint observer* is used by a controller to measure and control joint positions. Actuators might be coupled to rotational and prismatic joints of any arm, or wheels of a mobile vehicle. At this level, inverse kinematic models may also be used to permit reference commands to be specified in the end-effector coordinate frame. At the sensor level, the *feature-based observer* derives feature values and relations from measurement data and implements task control within the local feature domain. At the world level, the *recognition observer* interprets sensory features and develops a world frame model of the current task configuration. At each level the observer output combines the task goals and constraints to generate the new command structure.

Fig. 2 shows an example of a sensor-based control task in which a robot arm acquires an object from the table using visual feedback control. A task-level command specifies manipulation of the object; however, the robot has not been preprogrammed with knowledge of the object position. In this sense, the task environment is "unstructured." A television camera is attached to the robot arm and provides visual sensing capability. The image acquired by the camera must be processed by a computer vision system to identify the object and infer relationships between the spatial position of the object and the camera position. Such relative position information may be used to guide the robot to acquire the object from the table.

The same problem arises in the navigation of a mobile robot with respect to objects in an unstructured environment using visual feedback. The images acquired by the on-board camera (or cameras) provide cues to the relative position of the robot to objects in the environment. A local model is used to relate
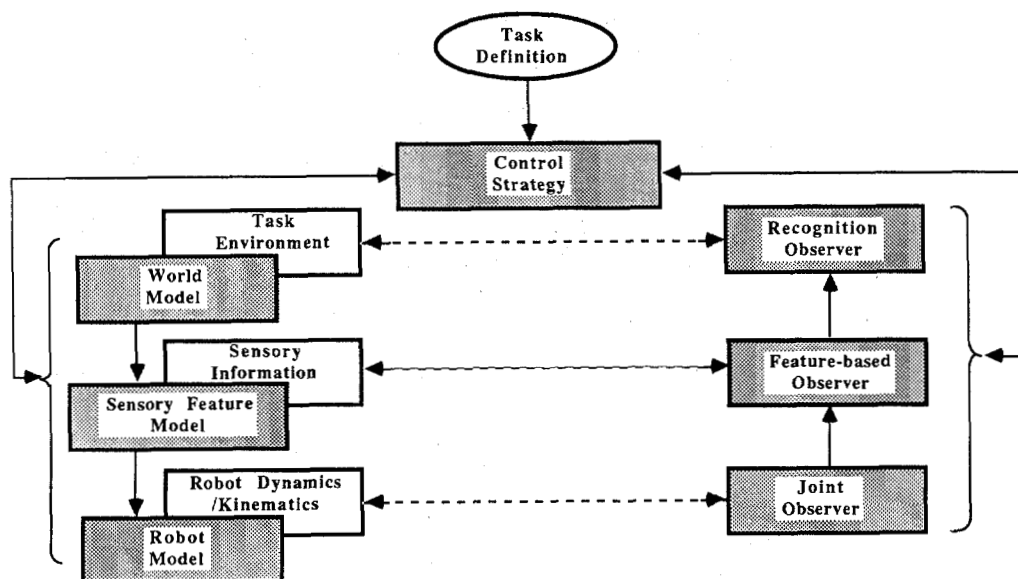
Fig. 1. Hierarchical sensor-based control.
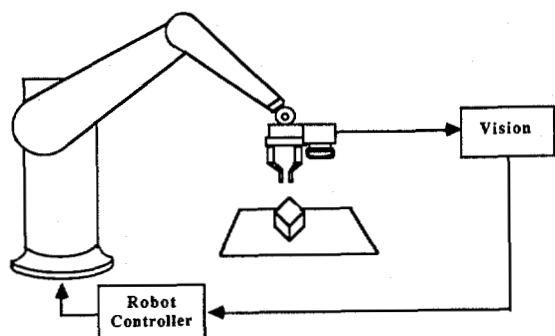
Fig. 2. Robot acquiring object using visual feedback.

image features to local robot motion, while a global model checks consistency of local interpretations [7], [4]. Such an image processing and motion-planning sequence constitutes a control loop which is coupled to both the local and global models. The dynamics of such a control structure depend critically on the local and global models of the robot, sensor, world reference frames, and their relationships. The distribution of control among these reference frames is important to achieve good dynamic performance as well as reliable navigation.

Analysis of these hierarchical control structures which couple robot motion to unstructured environments presents a number of key issues. In particular, the dynamic performance of the system is influenced by computational delays, uncertainty, robot dynamics, and coupling in the observer itself. In this paper we examine such issues for the case of visual servo control. A recognition observer is defined for a system which infers object position and orientation from a set of derived image features. The resulting "position-based" visual servo control system incorporates the interpretation phase into its primary feedback loop. In this paper, we focus on a feature-based observer which uses image features as a basis for a hierarchical control structure. Image features which are uniquely related to spatial position are used to define task

reference configurations and control robot actuators. Such an "image-based" visual servo control strategy offers advantages for reduced delay and estimation noise within a given recognition regime, as well as providing a novel "teach-by-showing" strategy for task specification.

Image-based visual servo control poses particular challenges to the observer/controller design to achieve consistent dynamics. The mapping between image features and the world coordinate frame may be unknown but dependent on the system configuration, as well as nonlinear and coupled. We have studied the application of an adaptive controller to achieve predictable and stable dynamic properties at this control level.

This paper first defines visual servo control structures, then focuses on the definition and control strategies for a sensor-level feedback system with image-based observer. Simulation studies demonstrate the performance of this control strategy for two- and three-degree-of-freedom systems.

II. VISUAL SERVO CONTROL

Fig. 3 illustrates a conventional robot arm positioning system which maps world coordinate frame reference signals X_{ref} into joint reference signals θ_{ref} using a kinematic arm model. The joint angle servo control system [19], [9], [25], [24], [20], [33], [5], [16], [18] uses a joint observer with position and velocity feedback to position the joint motors to the desired angles. The actual robot geometry may be slightly different than the robot model, and therefore the actual end-effector X may differ from the desired position X_{ref}. In real systems, there is no way to monitor this final positioning error since no measurement or feedback of final end-effector position is available. In this sense, the control loop is never closed around the end-effector position itself leading to inherent limitations in the ability of such a system to compensate for inaccurate modeling of the arm or to derive positioning error signals relative to unstructured environments.
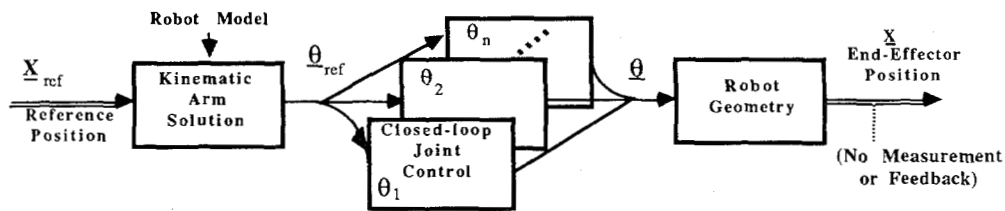
Fig. 3. Basic robot positioning control (vectors represented by underline).
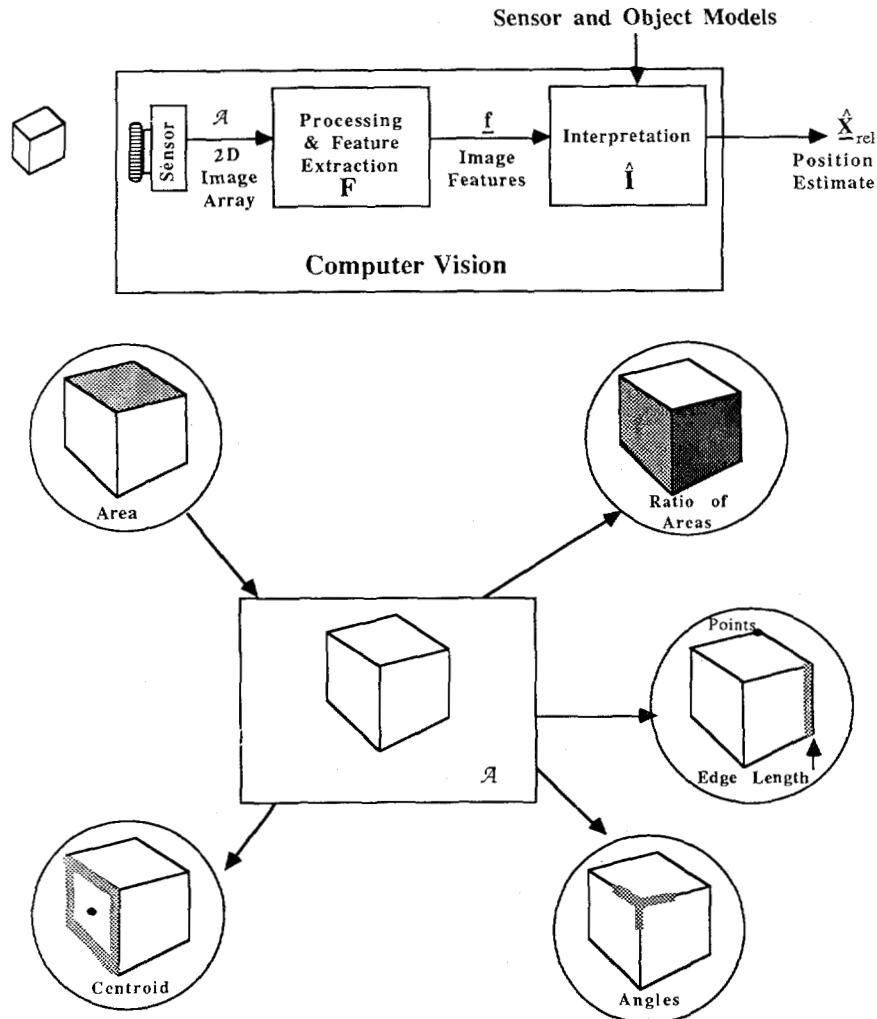

Fig. 4. Computer vision (vectors represented by underline).

The addition of visual sensing as a measurement system for relative end-effector position provides a basis for overcoming some of these limitations. However, the use of computer vision to infer position and orientation of objects, or interpret general three-dimensional relationships in a scene, is in general a complex task requiring extensive computing resources. Techniques which may exploit simpler sensors, structured lighting, or minimize processing for image interpretation may offer advantages for visual servo control implementations [1], [11].

Fig. 4 illustrates schematically an approach to the interpretation of a two-dimensional image for inference of three-dimensional position and orientation. In the block diagram, a sensor, such as a TV camera, is used to acquire a two-dimensional array $\mathcal{A}$ of brightness values from the three-dimensional scene. This image array may undergo various types of computer processing to enhance image properties and extract local and global image features. This feature set f typically includes relations among structural components of the image such as points, lines, and areas, as well as quantitative parameters attached to them. In reality there is a continuum of possible image features and their transformations, and their choice depends on the purpose and requirements of their subsequent use or interpretation. The image feature set f provides the basis for an *image-based* observer and associated feedback control structure. At a higher level, the image feature set f may be used to interpret the observed scene. Such an interpretation requires the recognition of
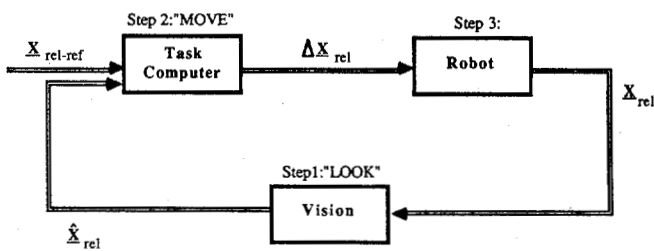
Fig. 5.   Static "look and move" control (vectors represented by underline).

objects in the scene and the estimate of object relations in the world coordinate frame. The output of this recognition observer is an estimate of the relative position of camera and object $\hat{X}_{rel}$ and may be used in a sensor-based feedback controller based on world coordinate reference signals $X_{rel-ref}$. Such a recognition observer depends on transducer, object, and scene models for its interpretation and may introduce complex forms of measurement noise as well as time delays into the feedback system.

Fig. 5 shows a simple example of a visual servo control structure based on the recognition observer. This system is called a position-based static "look and move" structure for visual servo control and is used most often in present industrial applications [30], [3], [12]. The system operation consists of a sequence of independent steps.

Step 1: The vision system "looks" at the scene, or object, and estimates the relative end-effector position $\hat{X}_{rel}$. In current applications the recognition and position measurement phases are relatively simple due to the highly structured environment.

Step 2: The position estimate is sent to a task computer. The task computer computes the difference ΔX between where the end-effector should be $X_{rel-ref}$ and the current position estimate. The task computer then issues a command to an independent closed-loop robot positioning system[1] to "move" by the incremental distance ΔX.

Step 3: The robot moves to the new position. Step 1 is not repeated until the robot completes the motion specified by the "move" command.

If the combined accuracy of the robot positioning and vision measurement systems are within the allowable tolerances of the task, then this sequence need only be executed once. However, if improved accuracy, noise reduction, rejection of external disturbances, or tracking of a moving object is required, then the sequence of operations is repeated until a specified accuracy is achieved. The static "look and move" structure demonstrates the concept of interactive sensing for robot positioning but is not a *dynamic* control system since each step is executed independently and in sequence. Thus the dynamics of each operation at each level of the hierarchy do not affect the overall system stability.

In contrast, if the visual feedback system is structured so that the three steps outlined are executed in parallel (i.e., positions estimates $\hat{X}_{rel}$ and position errors ΔX_{rel} are updated as fast as they are measured, and position corrections are commanded to the robot while it is moving), then the dynamic

interaction between the levels of the hierarchy becomes critical. Using this approach, dynamic visual servo control systems can be synthesized [1], [2], [31], [6]. The role of computer vision as the recognition observer affects the overall system dynamics, and a visual feedback controller is required for stability and to achieve acceptable transient response (Fig. 6). The linearity, noise properties, coupling, and computational delays of this measurement process become essential considerations for controller design. Formal analysis and design of feedback controllers for visual servoing using principles of control theory has not appeared in the literature except for a simple case [6]. Most visual servo controllers have been designed using *ad hoc* strategies [1].

This dynamic feedback strategy may further be generalized to control the open-loop dynamics and kinematics by direct joint activation. The digitally controlled position-based visual servoing structure (Fig. 7) may have potential advantages, including elimination of added computational delay, required by the "arm-solution" evaluation period, and elimination of "arm-solution" modeling inaccuracies. The feedback controller must compensate for any nonlinear and coupled robot dynamics and kinematics, as well as measurement delays and noise. While Koivo [15] and Takegaki [29] did not mention visual servoing, they did propose adaptive feedback controllers for such combined dynamic and kinematic control. Furthermore, Khatib [13] proposes task-level "operational space" (positional) control, using visual feedback, based on a nonlinear feedback controller.

Dynamic control has the potential to achieve faster responses than "static" systems, and dynamic considerations will become increasingly important as vision processing becomes faster and task representations more demanding. Dynamic visual servo control presents a variety of difficult design problems which are not currently addressed in the literature, including a formal approach to controller design and complexity of the feature-based or recognition observer. An adaptive image-based control approach to this problem is described below.

III. IMAGED-BASED CONTROL

In the position-based control approaches, the vision system is used as a recognition observer to measure the relative positions X_{rel} between the robot end-effector and some object in its environment. This measurement process can be decomposed into two nonlinear transformations. First, the transduction and feature extraction functions, or world-to-feature space transformation, can be viewed as the inverse of an ideal interpretation, in the absence of noise, according to

$$f = \mathbf{I}^{-1}[X_{rel}] \tag{1}$$

where f are the features and interpretation $\mathbf{I}$ is "ideal" in the sense of being based on exact object and image transducer models. Second, the features are mapped to world space by the approximate interpretation transformation:

$$\hat{X}_{rel} = \hat{\mathbf{I}}[f] \tag{2}$$

where modeling inaccuracies and image transducer noise lead

---

[1] The closed-loop robot positioning system includes dynamic joint servo controllers and kinematic decoupling software which allow movements to be specified in world or tool coordinates.
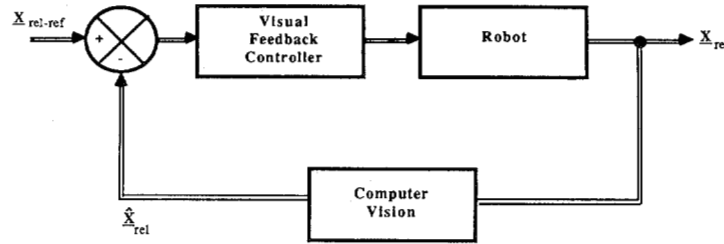
Fig. 6.   Dynamic visual servo control (vectors represented by underline).
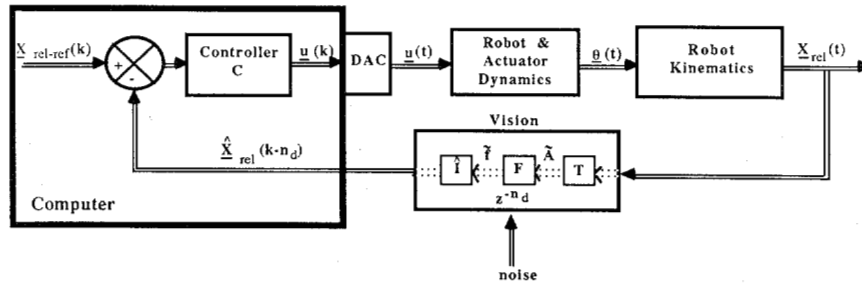
Fig. 7.   Position-based visual servoing (vectors represented by underline)

to equivalent measurement noise. If the interpretation has a unique inverse mapping, over the control region of interest, such that X_{rel} are single-valued functions of f, then this suggests that the system can be controlled, to unique end-points, using features directly as the feedback and reference signals, thus eliminating the interpretation step in (2). This feature-based observer approach relies on the systematic variation of image features with relative object position. Such a relationship is illustrated in Fig. 8. In this case, the task is specified by portraying the current camera image and the desired camera image. The image features corresponding to an image trajectory as the camera moves may be plotted as shown in the figure. Monotonic, although nonlinear, feature-to-position relations are obtained in this case using area, relative area, and center-of-gravity features. The uniqueness condition is satisfied, for the control region of interest, when [34] 1) the first partial derivatives of f are continuous, and 2) if the Jacobian of the ideal inverse interpretation is nonsingular; i.e.,

$$\det [J_{feat}] \neq 0 \qquad (3)$$

where J_{feat} defined as the feature sensitivity matrix is

$$\det \left\{ \frac{\partial \mathbf{I}^{-1}}{\partial X_{rel}} \right\} \doteq J_{feat}. \qquad (4)$$

In practice, J_{feat} can be estimated on-line to test the condition in (4). This condition must be true for both position and image-based approaches. Further, since the determinant is only defined for square matrices, then the permitted number of degrees-of-freedom must equal the number of measured features.

A digitally controlled image-based visual servo (IBVS) control structure, which uses feature feedback is represented in Fig. 9. This system was first proposed by Sanderson and Weiss [27]. In such an IBVS system, the reference and feedback signals are defined in terms of the image feature
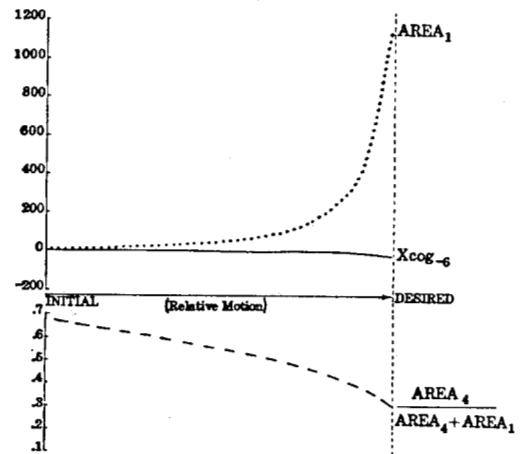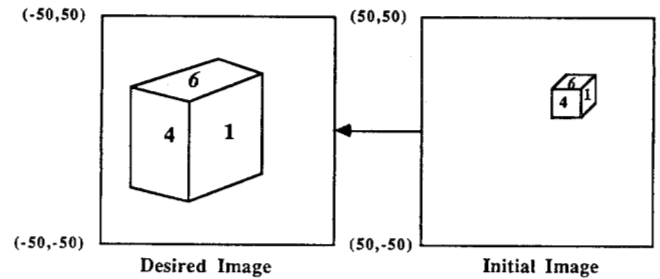
Fig. 8.   Features change with motion.

values corresponding to the current and desired robot positions. The feature errors may be derived at every measurement time and used to drive the robot in a direction which decreases the error. In Fig. 9, u are the control signals, θ are the robot joint coordinates, and n_d is the number of feedback delays introduced by the vision processing. The characteristics of each block are described in the next section. Image-based structures which incorporate inner closed-loop positioning
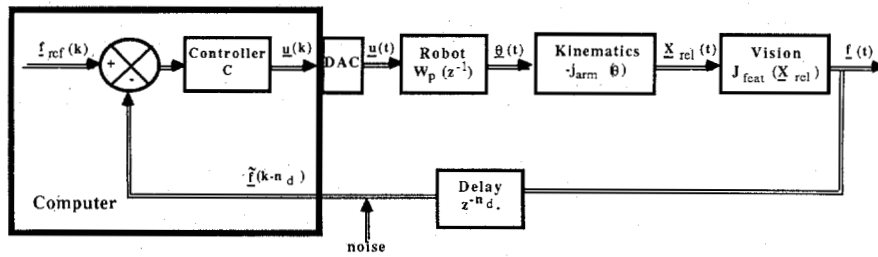
Fig. 9. Image-based visual servoing (vectors represented by underline).

control, such as in the position-based "look and move" structure, can also be derived.

In image-based control, reference signals $f_{ref}(k)$ must now be defined in feature-space. To accomplish this, the task could first be defined in world space $X_{rel-ref}$ and then mapped into f_{ref} according to an idealized inverse interpretation in (1). Equivalently, if $J_{feat}(X_{rel})$ is known or can be measured and the initial displacement X_{rel}° is known, then the feature signal can be derived by evaluating the feature sensitivity matrix along $X_{rel}^{\circ} + \delta X_{rel-ref}$ according to

$$\delta f_{ref} = J_{feat} \delta X_{rel}. \qquad (5)$$

While both approaches still require an interpretation procedure to recognize the features and to derive the transformations, they may offer potential advantages by eliminating inaccuracies of the actual interpretation, in the feedback path, and by requiring smaller sampling periods as a result of the elimination of the feedback interpretation delay.

An alternative approach, which only requires an interpretation procedure for feature recognition, is to define the reference signal directly in image feature space using a "teach-by-showing" strategy. In this approach, an image is transduced in the desired reference position and the corresponding extracted features represent the reference features. For repetitive tasks, with known world coordinate trajectories, the reference feature signals can be defined *a priori* as a "moving" or time-varying image along the path. In an unstructured task environment, only the final or desired feature values can be defined, and the world coordinate trajectory cannot be directly controlled. The most useful applications of teach-by-showing image-based systems might be for tasks requiring fast and accurate corrective motions, where the *exact path* is not critical (e.g., for precision assembly including random part acquisition and parts alignment). While the path cannot be explicitly controlled with the teach-by-showing strategy, a limiting case shows that if the coupled feature sensitivity matrix J_{feat} is constant, and each feature is specified to have identical time responses, the predicted path is straight-line, irrespective of the number of degrees-of-freedom (DOF). In addition, our simulation studies, to be described, show that smooth paths are achieved over a wide variety of system and parameter situations. The teach-by-showing approach presents additional requirements for controller design. In this approach, it is assumed that the inverse transformation I^{-1} is unknown. Therefore, the feedback controller must be based on a design approach which not only

compensates for the nonlinear and coupled properties of I^{-1}, but also for unknown values.

IV. CONTROL OF IMAGE-BASED SYSTEMS

The analysis, design, and evaluation of image-based systems has been studied by Weiss [32]. To design an image-based controller, it is useful to consider first the small-signal model (i.e., about a nominal operating point or trajectory) of the IBVS structure in Fig. 9. The control signals are applied through digital-to-analog converters (DAC's) which can be modeled by the cascade of an ideal impulse sampler and a zero-order hold with a saturation nonlinearity [21]. The system output is the undelayed feature, while the feedback path is modeled by discrete unit delays. Linearized open-loop robot dynamics [5], or equivalent linear I/0 models [28], are represented by the discrete-time Z transformation $W_p(z^{-1})$. The feedback path is characterized by an overall small-signal sensitivity matrix J given by

$$J \doteq J_{feat} J_{arm} \qquad (6)$$

where J_{arm} is the kinematic arm Jacobian. In addition to the control requirements of the robot dynamics, the design of the controller C also depends on the J sensitivity matrices, feedback delays, and measurement noise. The sensitivity matrices are nonlinear and coupled functions of θ and X_{rel}; thus J varies as θ varies, and feature-space transformations are manifested by time-varying open-loop gains. Predicted values of J can deviate from actual values due to inaccuracies in the modeling of the three-dimensional object and transduction process, and from drift and variation in the transducer parameters. At the extreme, the values may be completely unknown *a priori* when minimal knowledge of the inverse interpretation transformations I^{-1} are available, such as arises when task programming is limited to the teach-by-showing strategy. Fixed feedback controller designs have limitations in the control of such nonlinear and unknown systems. Even if the nonlinearities are known, a fixed controller design for these systems is a formidable engineering problem. In contrast, an adaptive approach to controller design appears to be applicable for these requirements. The IBVS controller design used in our research therefore emphasizes the adaptive approach.

A. Adaptive IBVS Control

In the context of joint-level control, a few researchers have evaluated the potential application of adaptive control to robotic manipulators [5], [8], [10], [14], [16], [18]. Adaptive
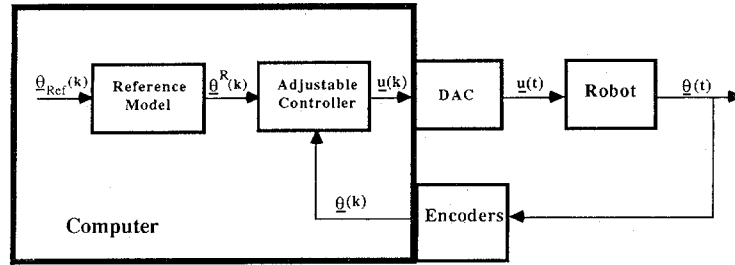
Fig. 10.   Model reference adaptive control (vectors represented by underline).

control has the potential to compensate for parameter uncertainty and variation over a wide range, while operating at high joint speeds. In these adaptive control schemes, an adjustable controller uses on-line identification to identify parameters of an equivalent input/output (I/0) linear model of the robot based on the I/0 information vectors $u(k)$ and $\theta(k)$ (i.e., actuator control signals and joint positions, respectively), under the assumption that the robot is linear and constant but has unknown parameters. An equivalent I/0 model is one that predicts the output $\theta(k)$ from past and present I/0 information independent of the physical model of the robot. The estimated parameter values are then used in a linear feedback controller as though they were the actual parameters.

The mathematical basis for our adaptive controller follows the enhanced identification error model reference adaptive control (MRAC) developed by Morris and Neuman [22]. While similar approaches have appeared in the literature, their research focused on details of physical implementation including control signal saturation, controller stability, measurement noise, and computational complexity for microprocessor implementation. Since the algorithm did not include control of systems with discrete measurement delays, we have extended it to include control of systems with delay [32]. Additional modifications for applying uncoupled MRAC to the control of coupled nonlinear systems were also developed.

In joint-level MRAC control (Fig. 10), the reference model output $\theta^R(k)$ specifies a stable and realizable closed-loop dynamic response of the output $\theta(k)$ to the reference signal $\theta_{ref}(k)$. The difference between the reference model output and the process is called the full-parallel (FP) output error:

$$e_0^{FP}(k) = \theta^R(k) - \theta(k). \tag{7}$$

The adjustable controller utilizes the identified parameters information to adjust the gains on-line to drive the FP error to zero, thus forcing the robot output to track the reference signal in accordance with the performance specified by the model. In the identification-error method of MRAC control [18] an identifier predicts the robot joint outputs, $t(k)$, based upon parameter estimates of an equivalent linear I/0 model. The identification error

$$e_{ID}(k) = \theta(k) - t(k) \tag{8}$$

drives the adjustment mechanism which updates the estimates of the equivalent parameters. These estimates are then used to adjust the gains of a linear controller which is driven by the model output. The adjustment mechanisms can be designed from either parametric optimization or stability viewpoints.

Both single-input single-output (SISO) and multiple-input multiple-output (MIMO) equivalent model formulations can be used to derive the adaptive controller. In the context of joint-level control, Neuman and Stone [23] have justified the latter modeling approach by demonstrating that individual joints of a coupled and nonlinear robot can be modeled by linear time-varying second-order SISO transfer functions. They show that the transfer function parameters vary smoothly in the work space as a function of the joint positions, velocities, and accelerations. Although MIMO controllers have a greater potential for decoupling a coupled system, they are computationally complex, and do not lend themselves to modularity. A modular system can easily be extended to increasing degrees-of-freedom and distributed processing. Uncoupled adaptive controllers have already demonstrated the potential to control dynamically coupled robots [16], [18] and would be easier to implement in current laboratory and factory computing environments. For these reasons, the approach which we developed emphasized uncoupled control of coupled systems, using the concept of equivalent SISO plants. For example, a two-degree-of-freedom IBVS system is controlled by two independent MRAC controllers, A_1 and A_2, in Fig. 11.

A SISO MRAC for a system with n_d unit feedback delays is summarized here. In our approach, we assume that the variable under control is the measurable, or delayed, feature signal $f_d(k)$. An mth order series-parallel reference model is described by the difference equation:

$$X_{SP}^R(k) = \left[\sum_{i=1}^{m} b_i^0 q^{-(i-1)} \right] f_{ref}(k) + \left[\sum_{i=1}^{m} a_i^0 q^{-(i-1)} \right] f_d(k) \tag{9}$$

where the delay operator q^{-i} is defined by

$$\{q^{-i}\}f(k) \doteq f(k-i). \tag{10}$$

In our studies we use second-order models (i.e., $m = 2$) with the model parameters selected to achieve critical damping. The two reference model poles, located at $z = e^{-\omega_n T}$, specify the desired closed-loop bandwidth ω_n of the system. The maximum bandwidth is constrained by the sampling period T according to the Nyquist criterion:

$$\frac{f_s}{f_{BW}} = \frac{1/T}{\omega_n/2\pi} = 2 \cdot PM \tag{11}$$

where a constant performance margin (PM) factor is included as a safety factor and to increase the sampling-to-bandwidth
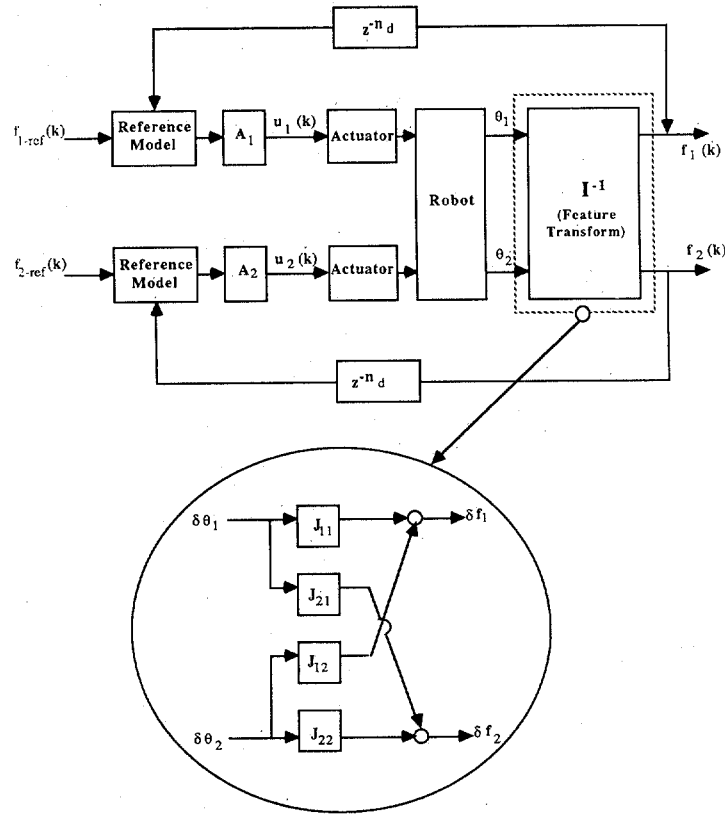
Fig. 11. MRAC control of IBVS system.

ratio so that the identifier can track the time-varying parameters.

We assume that system under control can be modeled by the nth order linear input/output equation

$$f_d(k) = \beta^T \Phi(k-1) \tag{12}$$

where the $(2n \times 1)$ information vector is

$$\Phi_d(k-1) \doteq [u(k-1-n_d)$$

$$\cdots u(k-n-n_d), f_d(k-1) \cdots f_d(k-n_d)]^T$$

and the $(2n \times 1)$ parameter vector is

$$\beta^T \doteq (b_1 \cdots b_n, a_1 \cdots a_n). \tag{13}$$

A series-parallel identifier predicts the delayed feature signal by

$$t_d(k) = \hat{\beta}^T(k-1-n_d)\Phi_d(k-1) \tag{14}$$

where $\hat{\beta}$ is the estimated parameter vector. The identification error is

$$e_{\text{ID}}(k) = f_d(k) - t_d(k). \tag{15}$$

A hyperstable adjustment mechanism [17] specifies the following identifier when the plant is assumed to be linear with *slowly* varying parameters:

$$\hat{\beta}(k-n_d) = \hat{\beta}(k-1-n_d) + \frac{1}{\lambda} P(k-1)\Phi_d(k-1)s(k) \tag{16}$$

$$s(k) = \frac{e_{\text{ID}}(k)}{1 + (1/\lambda)\Phi_d^T(k-1)P(k-1)\Phi_d(k-1)} \tag{17}$$

$$P(k) = \frac{1}{\lambda} P(k-1) - \frac{1 s(k)}{\lambda^2 e_{\text{ID}}(k)} P(k-1)$$

$$\cdot \Phi_d(k-1)\Phi_d^T(k-1)P(k-1) \tag{18}$$

where $P(k)$ is a $(2n \times 2n)$ adaptive gain matrix, $s(k)$ is the aposteriori error, and e_{ID} is the *a priori* error signal. The fading factor λ $(0 < \lambda \le 1)$ weighs past values of the input/output samples by the progression

$$1, \lambda, \lambda^2, \cdots, \lambda^k.$$

If $\lambda = 1$, new information is averaged with all past data, minimizing over reaction to measurement noise. If $\lambda \le 1$, old data are weighed less, and the mechanism can track the parameter β even when the parameters are slowly time-varying.

The controller is derived by solving (14) for the control signal $u(k)$ required to force the one-step ahead identifier output $t_d(k+1)$ to follow the reference signal $X^R(k)$. We do not use a predictor to estimate the actual, or undelayed, feature signal. Using this approach we can at best calculate what the control signal $u(k - n_d)$ should have been n_d sampling instants in the past and force the result to be $u(k)$. Inverting (14) for $u(k - n_d)$, and forcing the control signal to this value,

we obtain

$$u(k) = \frac{1}{\hat{b}_1(k - n_d)} \left\{ X_{SP}^R(k) \right.$$

$$- \left[\sum_{i=2}^{n} \hat{b}_i(k-1-n_d) q^{-(i-1+n_d)} \right] u(k)$$

$$\left. - \left[\sum_{i=1}^{n} \hat{a}_i(k-1-n_d) q^{-(i-1)} \right] y_d(k) \right\} .$$

$$(19)$$

A control penalty must be applied to (19) to ensure a stable and bounded control signal. A control signal penalty is obtained by multiplying (19) by the positive scaler $\pi(k)$ ($0 < \pi \le 1$). The penalty also reduces the effects of control signal saturation, noise, and underestimation of $\hat{b}_1$. To derive the control penalty, the Jury stability conditions are applied to test the location of the controller poles at each computational cycle. When pole magnitudes exceed the design parameter γ, where $0 < \gamma < 1$, the value of π is reduced until the poles lie within a circle of radius γ in the Z plane. In our studies we used second-order identifiers and assumed a single measurement delay (i.e., $n_d = 1$), thus the control penalty is computed as

$$\pi(k) = \begin{cases} 1, & \text{for } |\hat{b}^2/\hat{b}_1| < \gamma_2 \\ [\hat{b}_1(k)/\hat{b}_2(k)]\gamma^2, & \text{for } |\hat{b}_2/\hat{b}_1| > \gamma^2 \end{cases}. \quad (20)$$

B. Feature Selection and Assignment

Feature transformation coupling (i.e., represented by the small-signal feature sensitivity matrix J) leads to related problems of feature selection and assignment. Feature selection requires a subset of n features be selected from a set of m possible control features f_i ($i = 1, \cdots, m$), where $m > n$. Feature assignment addresses the choice of which feature should be used to control each actuator. Both issues are related to the degree-of-coupling of the feature transformation. We have developed a measure of coupling to address these issues.

1) Feature Assignment Using Diagonal Dominance: In applications where uncoupled controllers are used to control coupled plants, there is always the problem of choosing which servo error will control which actuator; that is, for a set of n outputs y_i ($i = 1, \cdots, n$), which servo error Δy_i should be filtered and coupled to the jth actuator as u_j? To formalize this assignment procedure let the open-loop linear system be defined by

$$Y(s) = H(s)u(s) \quad (21)$$

where $H(s)$ is an ($n \times n$) transfer function matrix. When the system is uncoupled, $H(s)$ can be transformed into a diagonal matrix by switching the jth and kth columns of $H(s)$, and therefore the jth and kth rows of $u(s)$, until all off-diagonal elements of $H(s)$ are zero. When $H(s)$ is diagonal, the only choice for servo error/actuator assignment is $u_i \leftarrow \Delta y_i$. When the system is coupled, then $H(s)$ cannot be transformed into a diagonal matrix by a simple row–column interchange. Servo

error/actuator assignment can be accomplished by organizing $H(s)$ in a "diagonally dominant" fashion [26], such that the diagonal elements dominate the off-diagonal elements. Diagonal dominance is defined as

$$|H_{ii}(s)| > \sum_{\substack{j=1 \\ j \ne i}}^{n} |H_{ij}(s)|, \qquad \text{for } i = 1, \cdots, n. \quad (22)$$

When $H(s)$ can be organized according to this definition of dominance, then limited stability properties of both coupled and uncoupled fixed control of the system can be formulated [26]. However, when applied to image-based systems, with $|JW_p| \leftarrow H(s)$, the sensitivity matrices may not satisfy this definition of dominance [32].

An alternative approach is to organize JW_p to maximize the inequality (22) over all possible column arrangements. This criterion reduces to defining the dimensionless measure of diagonal dominance as

$$D(k) = \log \sum_{\substack{i=1 \\ j \ne i}}^{n} \sum_{j=1}^{n} \frac{|JW_{p-ij}(k)|}{|JW_{p-ii}(k)|} \quad (23)$$

and then minimizing $D(JW_p)$ over all $n!$ possible column arrangements. The logarithm of the dominance is used since the ratios change by orders of magnitude.

2) Feature Selection: The image of a typical scene contains more features than there are degrees of freedom to control. The number of features must equal the number of degrees of freedom in an image-based system since the feature sensitivity matrix is constrained to be square. The possible number of ordered candidate feature subsets is

$$p(m, n) = \frac{m!}{(m - n)!} \quad (24)$$

where ordering is required to consider the feature/joint assignment.

To arrive at a criterion for feature selection, two aspects of feature-based control are analyzed:

1) the ability to specify world space path using feature-based trajectories (assuming that the control system can achieve a specified feature space performance), and
2) the control effort required to achieve the specified feature space dynamic performance.

It is shown below that the attributes of the feature sensitivity matrix J_{feat} relate to path performance, while the attributes of JW_p relate to the control effort aspects.

With respect to world space path, it is desirable to be able to control each world level degree of freedom (DOF) independently. To achieve this goal, an ideal subset of features should yield a feature sensitivity J_{feat} which is diagonal and constant. Then

$$\Delta X_i = \frac{\Delta f_i}{J_{feat-ii}} \quad (25)$$

where ΔX_i is the path error for the ith DOF, Δf_i is the ith

feature error, and $J_{\text{feat}-ii}$ is the (i, i)th element of J_{feat}. If straight-line motion is desirable, and all of the features exhibit the same dynamic response, then straight-line motion would be achieved. For example, assume that the ith feature response is specified by the critically damped response

$$f_i^0(t) \doteq f_i(t) - f_i(0) = \Delta f_i(1 - e^{-t/\tau}) \tag{26}$$

and all feature responses have the same time constant τ. The response of the ith DOF is

$$X_i^0(t) \doteq X_i(t) - X(0) = J_{\text{feat}-ii}^{-1} f_i^0(t). \tag{27}$$

The relationship between any two Cartesian degrees of freedom becomes

$$\frac{X_i^0}{X_j^0} = \frac{J_{\text{feat}-ii}^{-1} \Delta f_i}{J_{\text{feat}-jj}^{-1} \Delta f_j} \frac{1 - e^{-t/\tau}}{1 - e^{-t/\tau}} = \text{constant} \tag{28}$$

which is constant and specifies the equation of a straight line in Cartesian coordinates. It thus becomes straightforward to specify straight-line motion.

If an ideal feature sensitivity matrix could be synthesized, then it still remains to control the system dynamically to achieve the desired feature response. Attributes of the overall sensitivity JW_p can be used to describe the control effort required to achieve the desired response. Similar to the feature sensitivity attributes, the idealized overall sensitivity matrix should be diagonal and constant. Diagonalization permits the unqualified use of independent SISO controllers. In our experience, these idealized sensitivity attributes cannot be expected in practice. The degrees of freedom are coupled and the sensitivities typically vary with position. Feature sensitivity changes are minimized for small motion tasks, and for configurations with large lens magnifications. However, if the feature sensitivity were constant, but coupled, the predicted path would still be straight-line motion irrespective of the number of degrees-of-freedom. Since

$$X^0 = J_{\text{feat}}^{-1} f, \tag{29}$$

then

$$X_i^0 = (J_{\text{feat}-i1}^{-1} \Delta f_1 + \cdots + J_{\text{feat}-in}^{-1} \Delta f_n)(1 - e^{-t/\tau})$$

$$= K_i(1 - e^{-t/\tau}) \tag{30}$$

where K_i is a constant. The constant relationship between any two Cartesian DOF's becomes

$$X_i^0 / X_j^0 = K_i / K_j \tag{31}$$

which is the equation of a straight line.

Since we may not expect to find feature subsets which yield idealized sensitivity attributes, a feature selection strategy could seek a subset which best approximates these ideals; i.e., select features which minimize the coupling and sensitivity changes along a trajectory. In our research, the diagonal dominance measure, $D(JW_p)$, in (23), is used to quantify system coupling. The feature selection strategy then becomes

minimizing $D(JW_p)$ and $D(J_{\text{feat}})$ over the set of candidate features. By minimizing $D(JW_p)$, improved dynamic response is achieved with SISO controllers. By minimizing $D(J_{\text{feat}})$, closer to monotonic path performance may be expected. Each strategy may not produce mutually exclusive decisions, and arbitration between them would be based on the relative importance of each attribute. For example, a system could be feature uncoupled in the joint space of an articulated robot arm but not uncoupled in Cartesian space. Since the degree of coupling plays such an important role in the independent control approach, our initial research has focused on the evaluation of feature selection based on the minimization of $D(JW_p)$. These relationships between diagonal dominance and performance are born out by simulation experiments as described in the next section.

V. SIMULATION STUDIES

Adaptive IBVS systems are highly nonlinear, making it difficult to predict their potential performance analytically. Mainframe simulation studies were therefore used to evaluate IBVS control. The systems were modeled with progressively complex dynamics, kinematics, and feature coupling to understand their relative contributions to the control problem and system performance. Extensive studies have been completed for one-, two-, and three-DOF systems, and preliminary results are available for a five-DOF system. Performance limitations and application of fixed controllers were also evaluated using linear model following controllers (LMFC) [17]. Each LMFC is derived by fixing the gains of the adaptive controller to values derived from initial learning trials in the simulation experiments.

In these studies, the response to step-input feature reference signals, defined by the teach-by-showing strategy, provides a suitable measure of system performance. The reference model bandwidths were selected so that the sampling-to-bandwidth ratio f_s/f_{BW}, in (11) was at least 20. To simplify the feature selection/assignment process, the low-frequency or dc gain of W_p is used to calculate the coupling index D in (23). We observed that for a set of features, the feature/joint assignment remains constant over large regions of control for uncoupled kinematic configurations such as a Cartesian robot. For these configurations, off-line measurement of J in the initial image can be used to select a fixed assignment over the entire control trajectory. Off-line measurement to approximate J is accomplished by sequentially moving each robot joint by small increments, and measuring the accompanying change in features. For coupled kinematic configurations, such as an articulated arm, a feature/joint reassignment is predicted when controlling over large distances in space, and a fixed feature/joint assignment is only suitable for applications requiring small corrective motions. Feature selection can also be based on initial image coupling measures if the potential candidates have relatively small coupling values.

The imaging camera is modeled as a pinhole lens, and image features are derived from the idealized nondistorted two-dimensional image points. Image distortions are difficult to model and vary widely with lighting, transducer resolution, and linearity. Noisy imaging conditions are manifested as
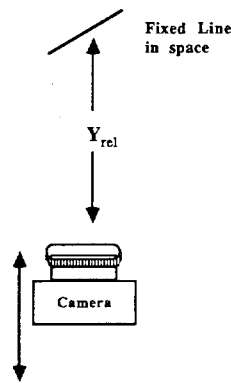
Fig. 12.   Single DOF.

measurement noise and modeled using varying levels of uniformly distributed noise added to the idealized extracted feature values. Some representative examples of adaptive IBVS control are discussed below.

A single DOF study incorporates a camera which moves relative to a fixed line (or edge) in space. The camera is mounted to a dynamically linear translational stage (Fig. 12), so that it is constrained to approach the line along a straight path. The control feature is the perceived line length. The feature sensitivity, over an 18-in excursion, is displayed in Fig. 13. The task is to move the camera from various initial starting positions to a desired position which is 1 in from the line. The final or desired position of the camera was specified to be in close proximity to the line to accentuate rapidly changing feature sensitivities as the camera approaches the object. The sampling period (for one frame time) is selected to be $T = 1/30$ s. In practice, if the vision system processing requires relatively long sampling periods, then higher sampling rate minor-loop velocity feedback controllers would be required to compensate for Coulomb friction, structural resonances, and to eliminate any apparent complex plane poles to satisfy the identifier's Nyquist sampling constraints. The fixed versus adaptive controller performance, as measured by position rise time, is also displayed in Fig. 13. While adaptive control performance remains constant over a wide range of excursions, fixed control response becomes sluggish. In general, a fixed controller tuned for one task may not be suitable for another task. A single adaptive controller is suitable for a range of tasks. Fixed controllers are suitable for tasks with small sensitivity changes (e.g., tasks requiring small corrective motion). While adaptive control is superior for large motions, our simulations also confirm the expected performance of the fixed controller: superior noise performance, and superior stability at lower sampling-to-bandwidth ratios.

Another simulation illustrates the performance of a system with nonlinear dynamics. The three-DOF revolute joint articulated arm, with a camera mounted to the third link, is shown in Fig. 14. In this example, the third joint θ_3 is not under visual servo control. This joint is automatically rotated such that the plane of the camera remains parallel to the robot base; i.e., $\theta_3(t) = -\theta_1(t) - \theta_2(t)$. The task is to move the camera relative to a fixed line in space. There are two control

features: the perceived centroid and line length. The coupling index is used to resolve the feature/joint assignment. Ranges of task motions included examples with initial-to-desired-position trajectories of short excursions (e.g., 1 in), to long-range motions of over 2 ft, and over a broad range of arm configurations. The dynamic robot model included Coriolis, centrifugal, viscous friction, and amplifier saturation effects. The simulated sample period was $T = 0.003$ s. An example is shown in Fig. 14 which displays the position trajectory of the camera and the corresponding rise times. In Fig. 14, the predicted trajectory is the path which would be achieved for perfect reference model following. The actual trajectory deviates from the predicted path due to initial transient identification errors which cannot be overcome in SISO control of the feature coupled system. The predicted trajectory deviates from a straight line by only 0.05 in. For larger motion tasks, we observed that deviations of the predicted paths from a straight line remain on the same order of magnitude, even though the feature sensitivities are tightly coupled and vary dramatically over the trajectory. Actual path deviations from the predicted trajectories were acceptable for the large motion tasks using a robot with linear uncoupled kinematics (e.g., $X - Y$ translational stages) under adaptive control. With fixed controllers, however, there were large path deviations and it was difficult to keep the line in the field of view. Using an articulated arm for tasks requiring larger motions, the additional kinematic coupling leads to unacceptably large path deviations with either adaptive or fixed SISO controllers. These systems would require a coupled controller.

A three-DOF configuration simulation consists of a stationary camera observing an object which is being moved. The object sits on top of a set of $X - Y - \theta$ translational and rotary stages (Fig. 15). The task is to move the object relative to the fixed camera position. The extracted features available for polyhedral objects (e.g., cubes, pyramids, wedges, etc.) include the centroid and area of each visible plane, and the relative areas between any two adjacent planes. For this configuration more features are available than degrees of freedom to control, and the coupling index is used to resolve both the feature selection and assignment. One method to evaluate the suitability of minimizing the coupling index to select features is to choose a very small motion task such that J, and thus $D(JW_p)$ stay essentially constant over the trajectory. System performance is evaluated for each possible combination of three features. For constant sensitivity, the $X - Y$ stage predicted path is a straight line, and path performance is evaluated by the deviation from a straight line. Dynamic performance is evaluated as the position rise time. For example, Fig. 16 summarizes the path and time performance as a function of the coupling index for 18 candidate feature subsets when a cube is used as the object. In this figure, the path performance is measured by the net distance traveled, where 0.144 in corresponds to the straight line. Fig. 17 displays the actual path and rotation responses for three of these subsets. Exhaustive testing, as represented by this example, shows that both path and dynamic performance improve as the coupling index decreases. For large motion tasks (e.g., trajectory greater than 1 ft), the observed paths

Feature Sensitivity   Fixed vs. Adaptive (BW=4.4 sec^{-1})
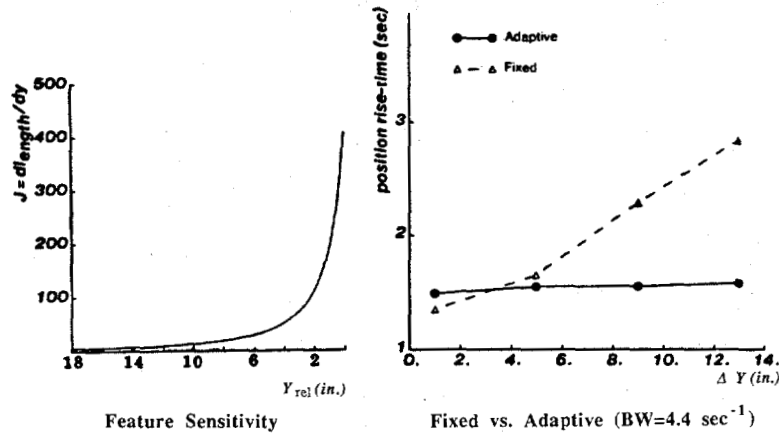
Fig. 13.   Single DOF performance.

(Features: length, X$_{cog}$)

Nonlinear coupled Kinematics
and dynamics
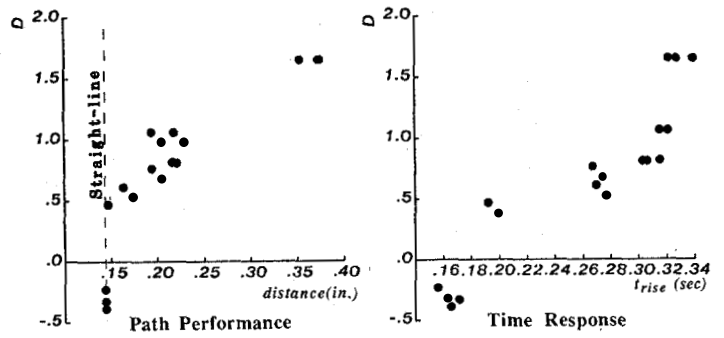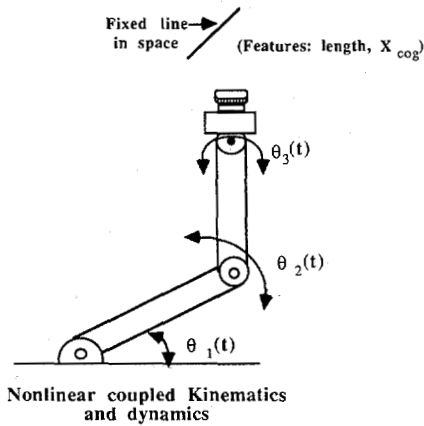
Fig. 16.   Performance versus coupling.
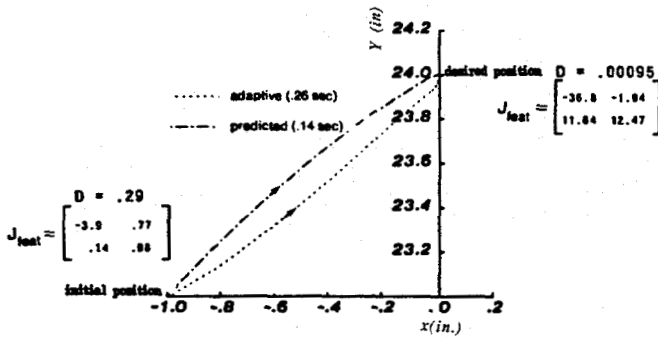
Fig. 14.   DOF task.
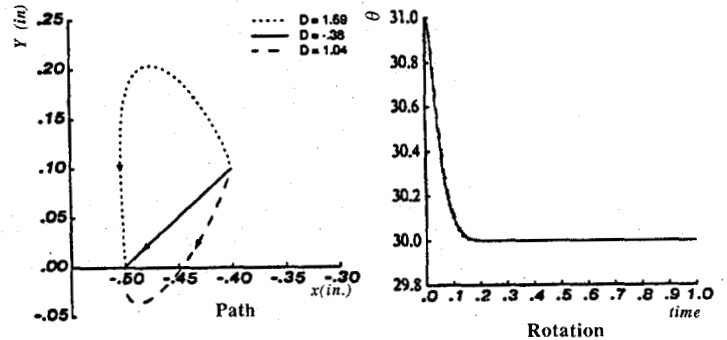
Fig. 17.   Three-DOF examples.
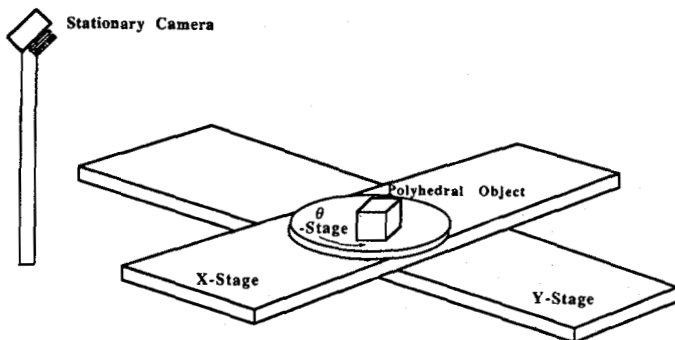
Fig. 15.   Three-DOF setup.

approach straight lines as features are selected which reduce system coupling.

We have also conducted preliminary simulation studies of IBVS control using a five-DOF system consisting of a camera mounted to the end of an articulated arm (e.g., as in Fig. 2) modeled with linear uncoupled dynamics. We used fixed proportional controllers, with gain adjustments and feature assignment/selection achieved by trial and error, to achieve stability with acceptable transient response and zero steady-state positional errors. While the predicted Cartesian paths were not derived, smooth joint motions were observed for properly tuned systems. It became difficult to tune the fixed controller for large motion trajectories because of the rapidly changing sensitivities and added kinematic coupling.

VI. DISCUSSION

In this paper we have described a hierarchical robot control structure with multiple observers and have pursued the analysis and simulation of a feature-based observer for visual feedback control. Evaluation of this adaptive image-based visual servo control strategy suggests that such systems may provide speed and accuracy improvements with simplified implementation. The feature-based strategy does not explicitly control position trajectories but may be regarded as an inherent strategy for real-time trajectory planning. The feature-based observer is useful in regimes of motion where image features have well-defined relations to the task. Such regimes must be monitored by a recognition observer within the hierarchical control structure. In a variety of applications this complementary relationship between feature-based and recognition observers occurs naturally in the task definition. In mobile robot navigation, for example, local features may be effectively used for real-time control, while global scene interpretation occurs at a much slower rate. Control of dexterous hands using finger-tip tactile arrays is another case where local or feature-based control may be used in a complementary fashion with a more global recognition observer to achieve complex manipulation capabilities yet maintain dynamic performance. The demonstration of an adaptive IBVS controller in this paper should provide insight and analytical tools for the analysis, design, and evaluation of dynamic sensor-based robot control systems and may serve as an example of a feature-based observer with broad application to hierarchical sensor-based systems.

REFERENCES

[1] G. J. Agin, "Real time control of a robot with a mobile camera," SRI International, Tech. Rep. 179, Feb. 1979.
[2] J. S. Albus, et al., "Hierarchical control for sensory interactive robots," in Proc. 11th Int. Symp. Industrial Robots, SME and RIA, Oct. 1981, pp. 497–505.
[3] J. Birk, et al., "General methods to enable robots with vision to acquire, orient, and transport workpieces," Univ. Rhode Island, Tech. Rep. 5, Aug. 1979.
[4] R. A. Brooks, "Solving the find-path problem by good representation of free space," in Proc. Nat. Conf. Artificial Intelligence, AAAI-82, Aug. 1982, pp. 381–386.
[5] M. J. Chung and C. S. G. Lee, "An adaptive control strategy for computer-based manipulators," Univ. of Michigan, Ann Arbor, Tech. Rep. 10-82, Aug. 1982.
[6] P. Y. Coulon and M. Nougaret, "Use of a TV camera system in closed-loop position control mechanisms," in International Trends in Manufacturing Technology: Robot Vision, A. Pugh, Ed. I.F.S. Publications Ltd., 1983.
[7] J. L. Crowley, "Navigation for an intelligent mobile robot," IEEE J. Robotics Automat., vol. RA-1, Mar. 1985.
[8] S. Dubowsky and D. T. DesForges, "The application of model-reference adaptive control to robotic manipulators," Trans. ASME, J. Dynamic Syst., Meas., Contr., vol. 101, pp. 193–200, Sept. 1979.
[9] J. M. Hollerbach, "A recursive Lagrangian formulation of manipulator dynamics and a comparative study of dynamics formulation complexity," IEEE Trans. Syst., Man, Cybern., vol. SMC-10, pp. 730–736, Nov. 1980.
[10] R. Horowitz and M. Tomizuka, "An adaptive control scheme for mechanical manipulators—Compensation of nonlinearity and decoupling control," in Winter Annual Meeting, Dynamics, Systems, and Control Div., ASME, Nov. 1980.
[11] T. Kanade and T. M. Sommer, "An optical proximity sensor for measuring surface position and orientation for robot manipulation," Carnegie–Mellon Univ., The Robotics Inst., Pittsburgh, PA, Tech. Rep. 83-15, Sept. 1983.
[12] S. Kashioka, et al., "An approach to the integrated intelligent robot with multiple sensory feedback: Visual recognition techniques," in Proc. 7th Int. Symp. Industrial Robots, SME and RIA, Oct. 1977, pp. 531–538.
[13] O. Khatib, "The potential field approach and operational space formulation in robot control," in Proc. 4th Yale Workshop on Applications of Adaptive Systems Theory, May 1985, pp. 208–214.
[14] A. J. Koivo and R. P. Paul, "Manipulator with self-tuning control," in Proc. IEEE Conf. Cybernetics and Society, 1980, pp. 1085–1089.
[15] A. J. Koivo and T. H. Guo, "Control of robotic manipulator with adaptive controller," in Proc. 20th IEEE Conf. Decision and Control. Dec. 1981.
[16] ——, "Adaptive linear controller for robotic manipulators," IEEE Trans. Automat. Contr., vol. AC-28, pp. 162–171, Feb. 1983.
[17] Y. D. Landau, Control and Systems Theory, vol. 8, Adaptive Control: The Model Approach. New York: Marcel Dekker, 1979.
[18] M. Le Borgne, J. M. Ibarra, and B. Espiau, "Adaptive control of high velocity manipulators," in Proc. 11th Int. Symp. Industrial Robots, Oct. 1981, pp. 227–236.
[19] C. S. G. Lee, "On the control of mechanical manipulators," in Proc. Sixth IFAC Conf. Estimation and Parameter Identification, June 1982, pp. 1454–1459.
[20] J. Y. S. Luh, "An anatomy of industrial robots and their controls," IEEE Trans. Automat. Contr., vol. AC-28, Feb. 1983.
[21] C. P. Neuman and C. S. Baradello, "Digital transfer functions for microcomputer control," IEEE Trans. Syst., Man, Cybern., vol. SMC-9, pp. 856–860, Dec. 1979.
[22] C. P. Neuman and R. L. Morris, "Classical control interpretation and design of microcomputer adaptive controllers," in Applications of Adaptive Control, K.S. Narendra and R. V. Monopoli, Eds. New York: Academic, 1980.
[23] C. P. Neuman and H. W. Stone, "MRAC control of robotic manipulators," in Proc. Third Yale Workshop on Applications of Adaptive System Theory. June 1983.
[24] R. P. Paul, Robot Manipulators: Mathematics, Programming, and Control. Cambridge, MA: MIT Press, 1981.
[25] M. H. Raibert and B. K. P. Horn, "Manipulator control using the configuration space method," Industrial Robot, vol. 5, pp. 69–73, June 1978.
[26] H. H. Rosenbrock, Computer-Aided Control System Design. New York: Academic, 1974.
[27] A. C. Sanderson and L. E. Weiss, "Image-based visual servo control of robots," presented at the 26th Annual SPIE Technical Symp., Aug. 1982.
[28] H. Stone and C. P. Neuman, "Dynamic modeling and adaptive control of a three DOF robotic manipulator," IEEE Trans. Syst., Man, Cybern., vol. SMC-14, July 1984.
[29] M. Takegaki and S. Arimoto, "An adaptive trajectory control of manipulators," Int. J. Control, vol. 34, pp. 219–230, 1981.
[30] K. Tani, et al., "High precision manipulators with visual sense," in Proc. 7th Int. Symp. Industrial Robots, SME and RIA, Oct. 1977, pp. 561–568.
[31] M. R. Ward, et al., "Consight: A practical vision-based robot guidance system," in Proc. 9th Int. Symp. Industrial Robots, SME and RIA, Mar. 1979, pp. 195–211.
[32] L. E. Weiss, "Dynamic visual servo control of robots: An adaptive image-based approach," Ph.D. dissertation, Carnegie-Mellon Univ., Pittsburgh, PA, 1984.
[33] S. J. Williams, "Frequency response multivariable robot control system design," in Proc. Inst. Elec. Eng. Colloq. "Control Theory in Robotics," Oct. 1983.
[34] C. R. Wylie, Advanced Engineering Mathematics. New York: McGraw-Hill, 1961.

Lee E. Weiss (S'79–M'82–S'83–M'83) received the B.S. degree in electrical engineering in 1972 from the University of Pittsburgh, Pittsburgh, PA, and the M.S. degree in bioengineering and the Ph.D. degree in electrical and computer engineering from Carnegie Mellon University, Pittsburgh, PA, in 1974 and 1984, respectively.

From 1974 to 1976 he was a Research Assistant associated with numerous Pittsburgh hospitals. During this period he was involved with the development of several prosthetic and implantable devices, and with the signal processing aspects of computerized fetal monitoring systems. From 1976 to 1979 he was a bioengineer at ARCO (Atlantic

Richfield) Medical Products Company where he was responsible for the design and manufacture of cardiac pacemaker heartleads. In 1979 he became the first graduate student to be supported by the Robotics Institute of Carnegie Mellon University, where he is currently a Research Scientist. He holds several patents in both the robotics and bioengineering fields. His research interests in robotics include dynamic sensory control, flexible assembly systems, automated inspection, and learning systems for automated workcells.
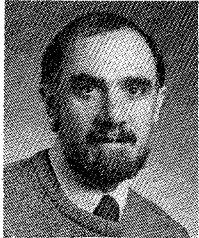
Arthur C. Sanderson (S'66-M'68-M'74-SM'86) received the B.S. degree from Brown University in 1968, and the M.S. and Ph.D. degrees in electrical engineering from Carnegie Mellon University, Pittsburgh, PA, in 1970 and 1972, respectively.

From 1968 to 1971 he was a Research Engineer at Westinghouse R&D Laboratories. During 1972–1973 he was a Postdoctoral Fellow at Delft University of Technology, The Netherlands, where he worked in the areas of neural modeling, pattern recognition, and signal processing. From 1975 to 1977 he was the Director of the Biomedical Engineering Program, Universidad Iberoamericana, Mexico City, Mexico. As Associate Director of The Robotics Institute at Carnegie Mellon University since 1980, he has played a principal role in establishing the Institute and coordinating its technical programs. He is currently on sabbatical leave from Carnegie Mellon University as Director of Information Sciences Research, Philips Laboratories, Briarcliff Manor, NY. He is the author of over 100 technical publications and proceedings. He is Associate Editor of the *IEEE Journal of Robotics and Automation* and Program Chairman for the 1987 IEEE International Conference on Robotics and Automation. His current research interests include planning systems in robotics, computer vision, sensor-based control, and flexible robotics assembly systems.

Charles P. Neuman (S'61-M'68-SM'78) is a Professor of Electrical and Computer Engineering at Carnegie Mellon University and a Member of the Robotics Institute. Dr. Neuman teaches undergraduate and graduate courses in control engineering. His current research interests include robotics; control engineering and adaptive control; control engineering applications of weighted residual methods; signal processing and numerical computation; sensitivity analysis and stability theory; and applied mathematics.

Dr. Neuman is an Associate Editor of the *IEEE Transactions on Systems, Man, and Cybernetics*, a member of the Editorial Boards of the *International Journal of Modelling and Simulation* and *Control and Computers*, and the United States Editor of *Electrosoft*. He is an IEEE Systems, Man, and Cybernetics Society TAB Representative to the Robotics and Automation Council. He is a member of SIAM, the Institute of Management Sciences, AAAS, Instrument Society of America (Senior Member), and Sigma Xi, Phi Kappa Phi, Tau Beta Pi, Eta Kappa Nu, and the Society of Harvard Engineers and Scientists. He is listed in *American Men and Women of Science, Who's Who in America, Who's Who in Frontiers of Science and Technology, Who's Who in Technology Today, Men of Achievement,* and the *World Directory of Mathematicians.*